Charge-Pumping Extraction Techniques for Hot-Carrier Induced Interface and Oxide Trap Spatial Distributions in MOSFETs

I. Starkov[1], H. Enichlmair[2], S. Tyaginov[3], and T. Grasser[3]
[1]Christian Doppler Laboratory for Reliability Issues in Microelectronics at
the Institute for Microelectronics, Vienna University of Technology, Gußhausstraße 27-29, A-1040 Vienna, Austria
[2]Process Development and Implementation Department,
Austriamicrosystems AG, Tobelbader Straße 30, A-8141 Unterpremstaetten, Austria
[3]Institute for Microelectronics, Vienna University of Technology, Gußhausstraße 27-29, A-1040 Vienna, Austria
Email: starkov@iue.tuwien.ac.at

***Abstract*—A thorough analysis of charge-pumping extraction techniques for hot-carrier induced defect spatial distribution in MOSFETs has been carried out. We discuss the main features of the existing approaches reflecting upon their shortcomings and applicability limits. For our investigations a new simple and accurate compact model for the MOSFET local oxide capacitance has been employed. The spatial distribution extracted from experiment is in a good agreement with the findings of our physics-based model of hot-carrier degradation.**

I. Introduction

To reveal and understand the physical picture behind hot-carrier degradation (HCD), it is essential to obtain quantitative information on the spatial distribution of hot-carrier induced interface states and oxide trapped charges (with densities N_{it} and N_{ot}) [1]. For this purpose, the charge-pumping (CP) technique proves to be a promising approach. Among numerous variations of the basic CP technique [2], the measurement method with varying amplitude (high/low-level) of the gate pulse is employed to obtain N_{it} and N_{ot} lateral profiles [3–6]. We present a careful study of the most widely used extraction techniques of spatial trap distributions from CP data, highlighting their limits of validity and linking them with our HCD model [7, 8] .

II. Experimental Support

We use a 5V n-MOSFET fabricated on a standard $0.35\mu\mathrm{m}$ CMOS process (Fig. 1). The lateral coordinate x refers to an origin placed at the left edge of the source contact. A device channel width of $W = 10\mu\mathrm{m}$ was chosen to obtain a sufficient charge pumping signal. Since we are dealing with a long-channel device (gate length $L_{\mathrm{g}} = 0.5\mu\mathrm{m}$) the worst-case conditions (WCC) of HCD are reached at $V_{\mathrm{gs}} = (0.4 \div 0.5)V_{\mathrm{ds}}$ [9]. This idea is supported by Fig. 2, demonstrating both experimental and simulated (with our HCD model [7, 10]) dependences of the WCC on V_{gs} and V_{ds}. The noise pronounced in the simulated curve is related to the stochastic nature of the transport kernel employed in our HCD model. Thus, we have intentionally chosen a stress regime close to the WCC (see checkpoint in Fig. 2) in order to maximize the contribution of all degradation effects. The device was stressed at $V_{\mathrm{ds}} = 6.5\mathrm{V}$, $V_{\mathrm{gs}} = 2.6\mathrm{V}$ and a temperature of $T = 40^{\mathrm{o}}\mathrm{C}$ for 10^5s. Such a temperature regime was used because trapping/detrapping in the oxide bulk is triggered by non-elastic trap-assisted tunneling which is accelerated at higher temperatures [11, 12]. In the inset of Fig. 2 the shift of the threshold voltage V_{th} vs. the stress time is depicted. One can see that the turn-around effect of the V_{th} shift [2, 13] is less pronounced at room temperature. These turn-around effects are related to a partial compensation of the charge stored in the oxide traps by interface state trapping [9]. In this context, the chuck temperature was set to $40^{\mathrm{o}}\mathrm{C}$ to accelerate the degradation processes.

We use an experimental scheme where the gate of the transistor is connected to a pulse generator, while source, drain and substrate contacts are grounded. As it was suggested in [5, 14], we measured the CP current at the drain ($I_{\mathrm{cp,d}}$), source ($I_{\mathrm{cp,s}}$) and substrate ($I_{\mathrm{cp,sub}}$). Due to the presence of the damage dose provided by the multiple-carrier component of the $\mathrm{Si-H}$ bond dissociation process [7, 15] it is important to perform separate current measurements. In other words, the assumption used in [3, 4] that the damage is induced only near the drain edge of the gate contact is incorrect. As a consequence, the drain component of the CP current can not be defined as

$$I_{\mathrm{cp,d}} = I_{\mathrm{cp,sub}}(\mathrm{stress}) - \frac{I_{\mathrm{cp,sub}}(\mathrm{fresh})}{2}. \quad (1)$$

The gate of the MOSFET was pulsed by a trapezoidal waveform at a frequency of $f = 100\mathrm{kHz}$. We use $V_{\mathrm{gl}} = 5\mathrm{V}$ and increase V_{gh} from -4 to 3V (varying high-level technique) and $V_{\mathrm{gh}} = 4\mathrm{V}$ with decreasing V_{gh} from 3 to -5V (varying low-level technique) in 0.02V increments, where V_{gl} and V_{gh} are the low and the high levels of the gate pulse, respectively (see Fig. 3). Such a small voltage step is required in order to obtain sufficient

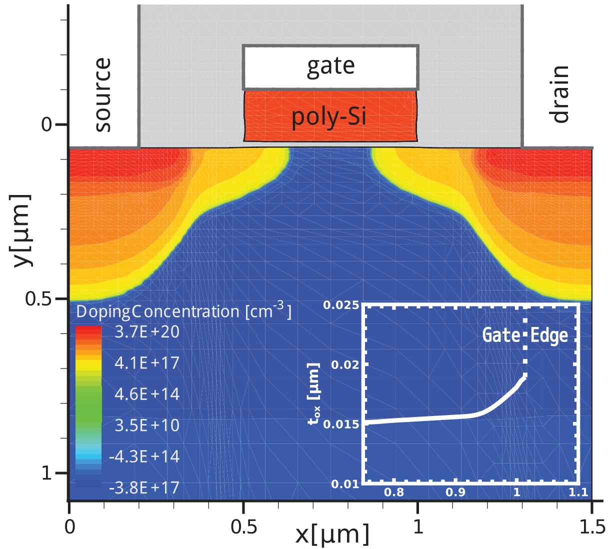

Fig. 1. The topology of the n-MOSFET with the net doping profile highlighted. Inset: the dependence of the oxide thickness vs. the lateral coordinate.

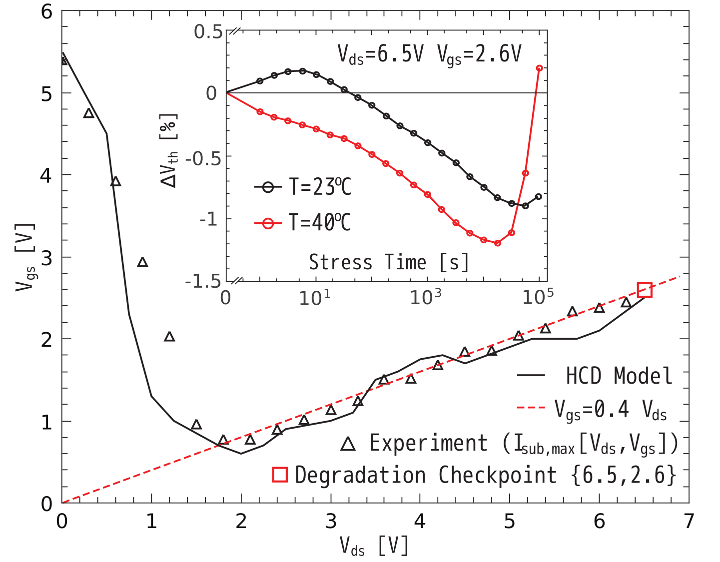

Fig. 2. The gate voltage as a function of the drain voltage corresponding to the worst-case conditions. Inset: the shift of $V_{\rm th}$ as a function of stress time at various temperatures

spatial resolution.

III. Defect Profiles Extraction Techniques

The lateral distribution of interface traps can be calculated as [16]

$$N_{\rm it}(x) = -\frac{1}{{\rm q}Wf}\frac{{\rm d}I_{\rm cp,d}(V_{\rm gh})}{{\rm d}V_{\rm gh}}\frac{{\rm d}V_{\rm th}(x)}{{\rm d}x} \tag{2}$$

in the case of varying high-level CP technique and

$$N_{\rm it}(x) = \frac{1}{{\rm q}Wf}\frac{{\rm d}I_{\rm cp,d}(V_{\rm gl})}{{\rm d}V_{\rm gl}}\frac{{\rm d}V_{\rm fb}(x)}{{\rm d}x} \tag{3}$$

in the case of varying low-level CP technique (q is the elementary charge). Here $V_{\rm th}(x)$ and $V_{\rm fb}(x)$ are the local threshold and flatband voltages [2]. If the influence of the interplay between oxide and interface charges is small enough, the $V_{\rm th}(x)$ and $V_{\rm fb}(x)$ keep the initial form corresponding to an undamaged device during hot-carrier stress. Otherwise necessary corrections of the $V_{\rm th}(x)$ and $V_{\rm fb}(x)$ after each stress time step have to be performed [3, 5, 6]

$$\begin{aligned} V_{\rm th,s}(x) &= V_{\rm th}(x) - \frac{{\rm q}\Delta N_{\rm ot}(x)}{C_{\rm ox}} + \frac{{\rm q}\Delta N_{\rm it}(x)}{2C_{\rm ox}} \\ V_{\rm fb,s}(x) &= V_{\rm fb}(x) - \frac{{\rm q}\Delta N_{\rm ot}(x)}{C_{\rm ox}} - \frac{{\rm q}\Delta N_{\rm it}(x)}{2C_{\rm ox}}, \end{aligned} \tag{4}$$

where $\Delta N_{\rm it}(x)$ and $\Delta N_{\rm ot}(x)$ is the change between pre- and post-stress concentrations of interface traps and bulk oxide charges. Parameter $C_{\rm ox}$ is the oxide capacitance per unit area and will be described below. The coefficient 2 in the denominator of the last term in (4) is noteworthy. The interface states are assumed to obey a homogeneous distribution over energy in the band-gap [6, 17]. Also, traps situated above mid-gap assumed to be acceptor-like while those in the lower half of the band-gap are donor-like. In the case of an n-MOSFET with a positive bias applied to the gate, the net charge is negative. The reason behind this is the charging of the acceptor-like interface states. Not disposing at the real distribution of traps over energy it is suggested that the charge stored in these states is $Q_{\rm it} = -{\rm q}N_{\rm it}({\rm q})/2$, thereby considering a uniform distribution.

In the case of the absence of significant amount of oxide charges generated under hot-carrier stress it is possible to use a simplified method for $N_{\rm it}$ extraction and consider only the effect of $N_{\rm it}$ on the calculated $V_{\rm th}$. In other words, only varying high-level or varying low-level CP technique can be used [7, 18].

All approaches described below have been developed to obtain the spatial distribution of both types of defects ($N_{\rm ot}(x)$ and $N_{\rm it}(x)$) induced by HCD. We discuss four main concepts for the characterization of the interface states and oxide-trapped charges in MOSFETs: Lee's [3], Li's [4], Chim's [5] and Mahapatra's [6]. Further, we emphasize the key issues of these extraction procedures. Aforementioned extraction techniques assume that each value of the transistor's local threshold and flatband voltage corresponds to only one position of the coordinate x before and after stress. That is, the effect of trapped charges on the $V_{\rm th}(x)$ and $V_{\rm fb}(x)$ distributions is one dimensional - the shift of the local threshold and flatband voltages at channel position x can be induced only by the charges at position x. This assumption can be additionally examined by using a modified charge-pumping

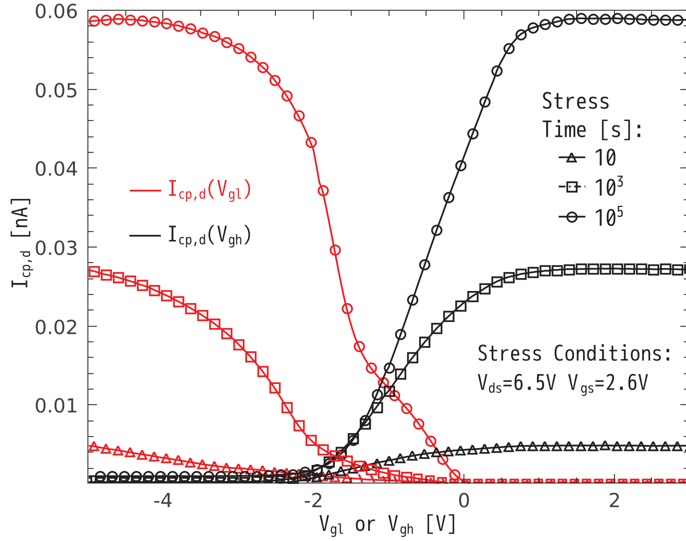

Fig. 3. Time evolution of the measured charge-pumping current during hot-carrier stress using the varying high/low-level charge-pumping technique.

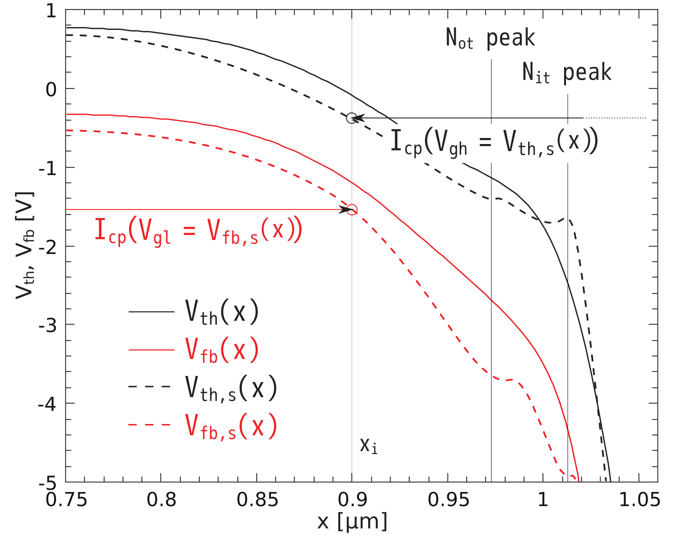

Fig. 4. Typical local threshold and flatband voltage profiles before $V_{\mathrm{th}}(x), V_{\mathrm{fb}}(x)$ and after $V_{\mathrm{th,s}}(x), V_{\mathrm{fb,s}}(x)$ hot-carrier stress for n-type MOSFET.

technique with both the high level V_{gh} and low level V_{gl} of the applied gate pulse are alternating during measurements [5, 14]. However, the investigation of the modified CP experimental schemes for verification of this assumption is out of the scope of this paper.

All considered methods employ the oxide capacitance C_{ox} as a crucial parameter of the extraction procedure. In the methods derived by Mahapatra [6] and by Li [4], C_{ox} is treated as a constant

$$C_{\mathrm{ox}} = \frac{\varepsilon_{\mathrm{ox}}}{t_{\mathrm{ox}}}, \tag{5}$$

where t_{ox} is the oxide thickness at the device center and $\varepsilon_{\mathrm{ox}}$ the dielectric permittivity. However, recently we have demonstrated that the coordinate dependence $C_{\mathrm{ox}}(x)$ due to the fringing effect is essential [19]. To account for the electric field non-uniformity near the source/drain ends of the gate the conformal-mapping method has been employed [20].

The local oxide capacitance can be written as parametric system

$$\left.\begin{aligned} x &= \frac{t_{\mathrm{ox}}(x)}{\pi}(\varphi + \exp(\varphi)) \\ C_{\mathrm{ox}}(x) &= \frac{\varepsilon_{\mathrm{ox}}}{t_{\mathrm{ox}}(x)(1+\exp(\varphi))} \end{aligned}\right\} \tag{6}$$

At $x \to -\infty$ (or $\varphi \to -\infty$) equation (6) asymptotically turns into expression for the parallel-plate capacitance (5).

To simulate the local oxide capacitance we employ the method developed by Lee *et al.* [3]. The presence of a probe uniform oxide charge $Q_{\mathrm{ot,uniform}}$ leads to a local threshold voltage shift $\Delta V_{\mathrm{th,uniform}}(x) = V_{\mathrm{th,s(uniform)}}(x) - V_{\mathrm{th}}(x)$ [3]. The local oxide

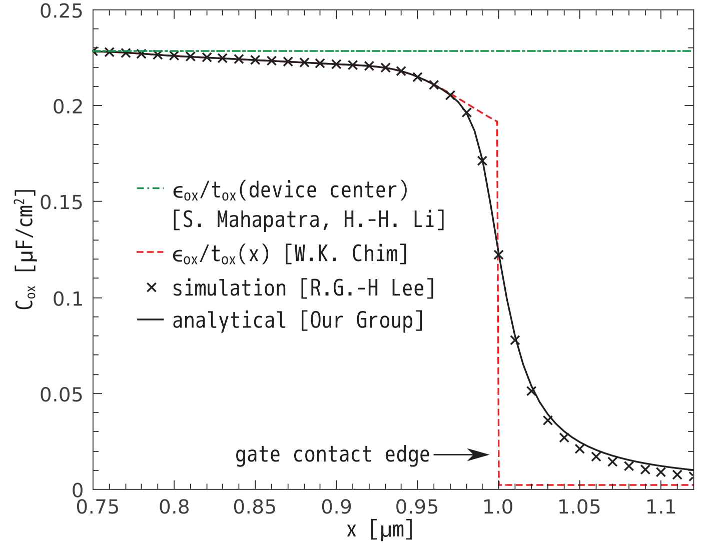

Fig. 5. The local oxide capacitance calculated using the approach of [3], compared with the newly developed analytical model [19].

capacitance is thus found as

$$C_{\mathrm{ox}}(x) = -\frac{Q_{\mathrm{ot,uniform}}}{\Delta V_{\mathrm{th,uniform}}(x)}. \tag{7}$$

The comparison of the simulations based on the method suggested in [3] and the analytical approach developed by our group [19] for $C_{\mathrm{ox}}(x)$ profile is presented in Fig. 5, demonstrating good agreement. At the same time, the expression (5) even when corrected

for $t_{\rm ox} = t_{\rm ox}(x)$ (Fig. 1, inset) [5] leads to a substantially different results. An abrupt reduction in $C_{\rm ox}(x)$ at the drain edge of the gate ($x = 1.0\mu$m) is unphysical and this approach should not be used in extraction algorithms. The spurious result produced with the method ignoring the $C_{\rm ox}(x)$ distribution may lead to an ambiguous picture of HCD [19]. Therefore, further in our investigations we use our model for the local oxide capacitance implemented in all considered characterization methods.

We point out here the crucial features of listed extraction techniques:

A. Chim's Approach

This extraction algorithm is based on the iterative correction scheme employing the equation system (4). The pre-stress CP edge is corrected for the additional charges associated with both $N_{\rm ot}$ and $N_{\rm it}$ generated due to the stress. For each position x_i, the maximum possible range where the post-stress local threshold voltage can lie is found. By comparing the varying pulse-high and varying pulse-low measured CP currents under consideration of chosen $V_{\rm th}(x_i)$ value from this range, $N_{\rm it}$ is separated from $N_{\rm ot}$. Namely, for assumed $V_{\rm th}(x_i)$ using (2) the $N_{\rm it}(x_i)$ is calculated. Further, for a known value of the interface state density at x_i, the local flatband voltage $V_{\rm fb}(x_i)$ is found employing (3). The obtained results are $I_{\rm cp}(V_{\rm gh} = V_{\rm th}(x_i))$ and $I_{\rm cp}(V_{\rm gl} = V_{\rm fb}(x_i)$. Since the maximum value of the CP current $I_{\rm cp,max}$ is the same for both varying high/low-level measurements (the effective channel length is the same), the following condition must be satisfied (see, Fig. 4)

$$I_{\rm cp,max} = I_{\rm cp}(V_{\rm gh} = V_{\rm th}(x_i)) + I_{\rm cp}(V_{\rm gl} = V_{\rm fb}(x_i)) \quad (8)$$

If (8) is not satisfied, then the chosen $V_{\rm th}(x_i)$ value is incorrect and it is necessary to repeat these steps from the beginning. Otherwise, a solution is found and we go to the next coordinate x_{i+1}.

B. Mahapatra's Approach

Here it is assumed that $N_{\rm it}(x)$ follows the lateral electric field distribution along the channel. The main idea is that the damage profile can be modeled best as Gaussian. However, a Gaussian distribution is inconvenient for analytical modeling because the integral results in the error-function. Therefore, the authors suggest to model the $N_{\rm it}$ profile by an analytically integrable function with similar shape

$$N_{\rm it}(x) = \frac{N_{\rm it,p}}{\cosh^2\left(\alpha[x - x_{\rm p}]\right)} \quad (9)$$

where $N_{\rm it,p}$ is the peak value of damage, $x_{\rm p}$ is the position of the peak along the channel and α is a parameter responsible for the spatial spread of the damage. This number of parameters is defined by the fitting procedure of experimental CP data. Implementation of (9) in system (4) significantly simplifies the extraction process.

C. Lee's Approach

In this routine, it is supposed that the hot-carrier induced impact on $V_{\rm th}(x)$ for the damaged region near the drain side can be empirically represented as

$$V_{\rm th,s} = \frac{V_{\rm th}(x_2) - V_{\rm th}(x_1)}{\ln(1 - (x_2 - x_1)/A)} \cdot \ln\left(1 - \frac{(x - x_1)}{A}\right) + V_{\rm th}(x_1), \quad (10)$$

while the undamaged region remains unchanged as $V_{\rm th}(x)$. Here $x_{1,2}$ are the boundaries of the damaged oxide region (defined by the evolution of the derivative of the charge-pumping curve with the stress time) and A is the only unknown variable to be determined by the optimization technique. As in Mahapatra's approach, employing of (10) in (4) results in a simplified defect profile characterization.

D. Li's Approach

This technique stands out against the others because it requires only varying high-level measurements. It is derived from the Shockley-Read-Hall theory which is used for the analytic charge-pumping current model. According to this model, $N_{\rm it}(x)$ is

$$N_{\rm it}(x) \simeq \frac{I_{\rm cp}(V_{\rm gl,2}) - I_{\rm cp}(V_{\rm gl,1})}{2k_{\rm B}TWfB\int_0^\infty (F(V_{\rm gl,1},t) - F(V_{\rm gl,2},t))\mathrm{d}t} \quad (11)$$

with $B \equiv \log(\sigma_{\rm n0}t_{\rm eme}(x)/\sigma_{\rm p0}t_{\rm emh}(x))$. Here $t_{\rm eme}(t_{\rm emh})$ is the non-steady-state electron (hole) emission time measured from two low gate voltages ($V_{\rm gl,1}$ and $V_{\rm gl,2}$). The fitting function F is obtained using device simulation and is equal to 1 at the center of the channel and rapidly decreases to 0 at near source/drain junction. The oxide-trapped charge density is derived as $N_{\rm ot}(x) = \Delta V_{\rm c}C_{\rm ox}$, where $V_{\rm c}$ is the difference of the voltage related to the half-maximum value of the $\Delta I_{\rm cp}/f - V_{\rm gh}$curves.

IV. Results and Discussion

The profiles extracted for stress time of 10^3s and 10^5s are depicted in Figs. 6,7 and Figs. 8,9. The extracted $N_{\rm it}(x)$ and $N_{\rm ot}(x)$ dependences were subjected to further validation as input data of the device simulator MiniMOS-NT [21] to model the transfer characteristics of the degraded device. Comparison of simulated and experimental curves demonstrates the applicability of the considered techniques (see Fig. 10).

One can see that the $I_{\rm d} - V_{\rm ds}$ dependence evaluated with Li's model spuriously overestimates the damage as compared to other extraction schemes. This fact can be explained by the necessity of the F function recalculation after each time iteration with erroneously localized $N_{\rm ot}(x)$ profile as input parameter. As it was mentioned above, spatial distribution of the oxide traps is defined using the change of half maximum of the charge-pumping curve. Such a variation is a very insensitive parameter and, as a consequence, the technique for calculating $N_{\rm it}$ and $N_{\rm ot}$ which is self-consistent, makes it questionable whether such additional

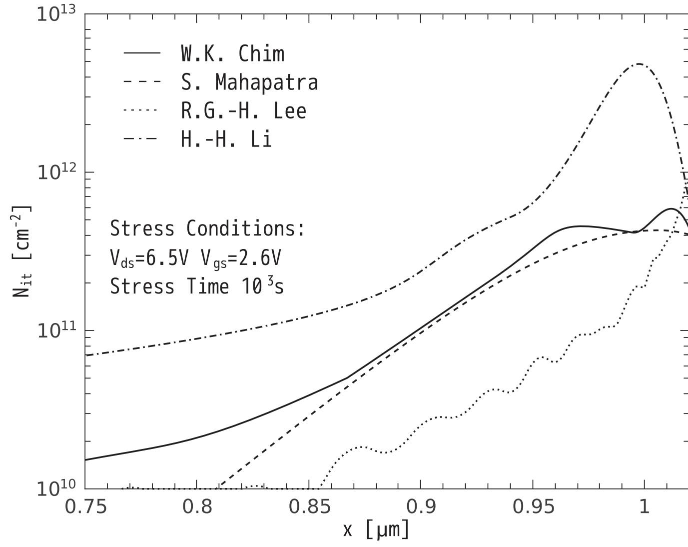

Fig. 6. The lateral distributions of $N_{\rm it}(x)$ and $N_{\rm ot}(x)$ calculated using different extraction approaches for 10^3s at $V_{\rm ds}$=6.5V and $V_{\rm gs}$=2.6V.

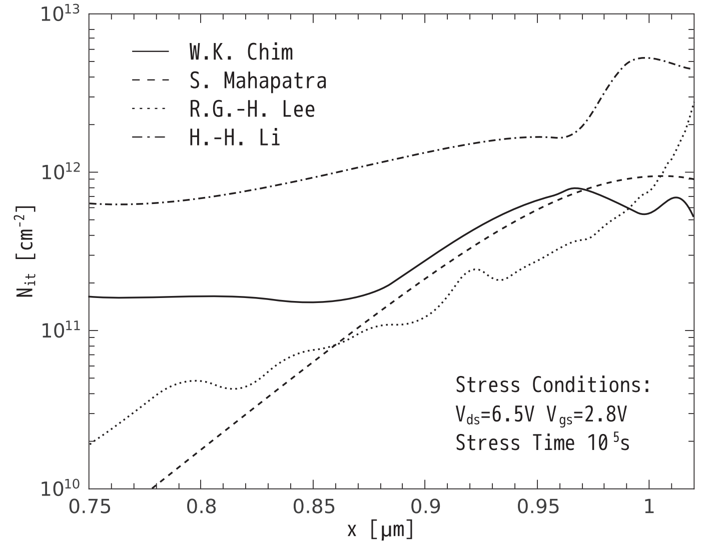

Fig. 8. The lateral distributions of $N_{\rm it}(x)$ calculated using different extraction approaches for 10^5s at $V_{\rm ds}$=6.5V and $V_{\rm gs}$=2.6V.

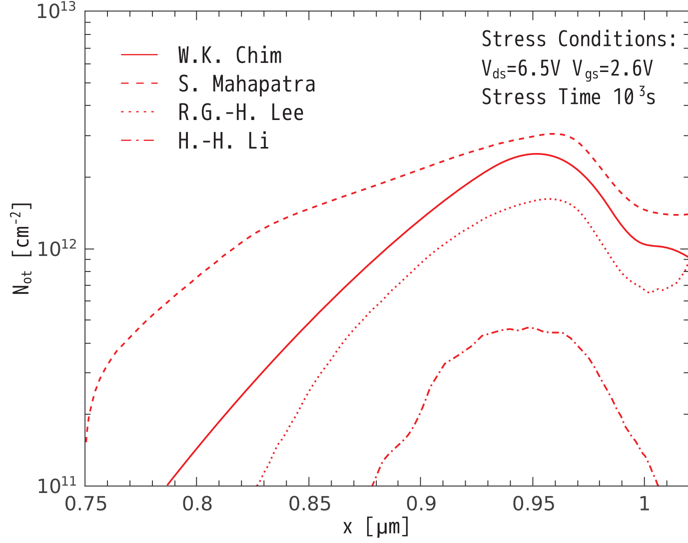

Fig. 7. The lateral distributions of $N_{\rm ot}(x)$ calculated using different extraction approaches for 10^3s at $V_{\rm ds}$=6.5V and $V_{\rm gs}$=2.6V.

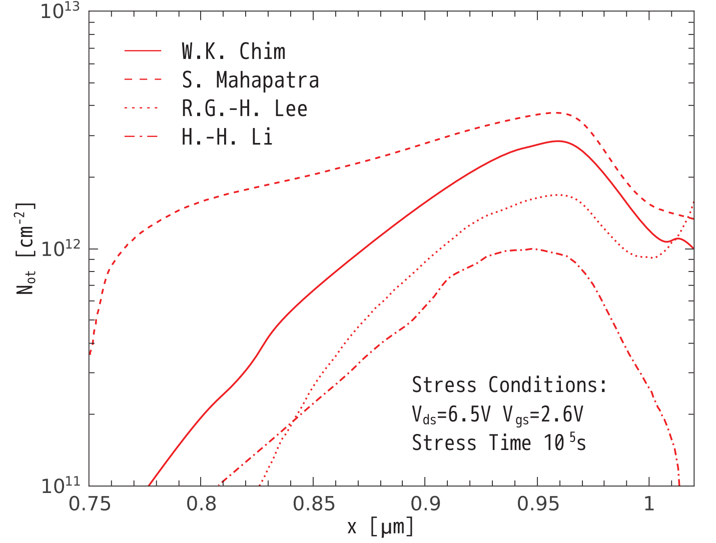

Fig. 9. The lateral distributions of $N_{\rm ot}(x)$ calculated using different extraction approaches for 10^5s at $V_{\rm ds}$=6.5V and $V_{\rm gs}$=2.6V.

efforts are justified [17]. At the same time, Mahapatra's approach predicts transfer curve degradation close to the result obtained by Lee's method but not strong enough as compared to the experimental data. In literature one may find different criteria how efficiently carriers interact with the bond, i.e. the maximum of the electric field, the carrier dynamic temperature, etc [9]. However, as we showed in [7], the $N_{\rm it}$ peak just corresponds to the maximum of the acceleration integral and is shifted away with respect to maxima of other quantities. As a consequence, for a proper HCD modeling it is not possible to use a simple analytical expression, like in (9,10). It is important to emphasize that the $N_{\rm it}(x)$ profiles extracted within Chim's technique features two peaks, see Figs. 6,8. This finding is in good agreement with the results of our HCD model [8] which shows that these peaks are related to the contributions induced by primary channel electrons and secondary generated holes (the second one is shifted towards the source) and correspond to the maxima of the electron and hole acceleration integrals [13]. Moreover, in our previous works

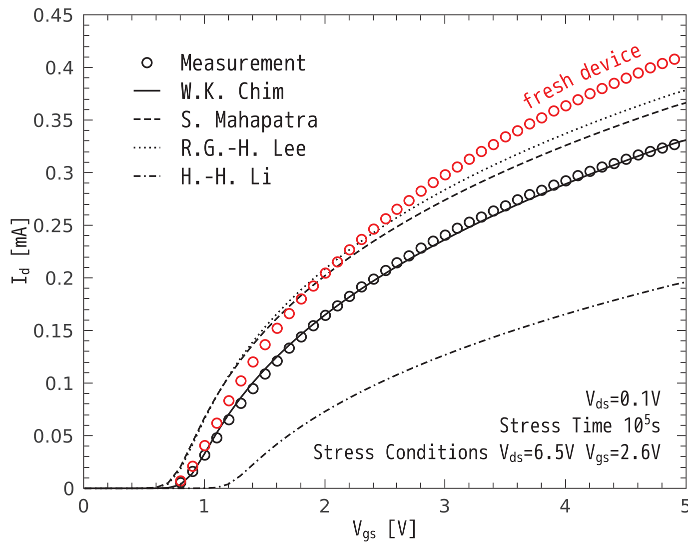

Fig. 10. The comparison of the experimental and simulated transfer characteristics for fresh and stressed devices. One can clearly see the applicability of Chim's technique.

[7] we have already demonstrated that in long-channel devices the multiple-carrier process of Si-H bond-breakage leads to $N_{\rm it}$ homogeneously distributed over interface which is confirmed in Fig. 8 ($N_{\rm it}$ plateau at the center of the gate).

V. Conclusion

An exhaustive analysis and comparison of extraction techniques of the hot-carrier induced interface and oxide trap spatial distributions were performed. We have emphasized a number of factors responsible for the accuracy of the extraction algorithms. Our investigations were performed using our newly developed HCD model. The advantages and limitations of the characterization algorithms improved by a new simple compact model for local oxide capacitance were discussed. Verification of the obtained results was performed using MiniMOS-NT simulations.

References

[1] A. Schwerin, W. Hänsch, and W. Weber, "The relationsjip between the oxide charge and device degradation: a comparative study of n- and p-channel MOSFETs," *IEEE Trans. Electron Dev.*, vol. 34, no. 12, pp. 2493–2500, 1987.

[2] P. Heremans, J. Witters, G. Groeseneken, and H. Maes, "Analysis of the charge pumping technique and its application for the evaluation of the MOSFET degradation," *IEEE Trans. Electron Dev.*, vol. 36, p. 1318, 1989.

[3] R. G.-H. Lee, J.-S. Su, and S. S. Chung, "A new method for characterizing the spatial distributions of interface states and oxide-trapped charges in LDD n-MOSFETs," *IEEE Trans. Electron Dev.*, vol. 43, no. 1, pp. 81–89, 1996.

[4] H.-H. Li, Y.-L. Chu, and C.-Y. Wu, "A novel charge-pumping method for extracting the lateral distributions of interface-trap and effective oxide-trapped charge densities in MOSFET devices," *IEEE Trans. Electron Dev.*, vol. 44, no. 5, pp. 782–791, may 1997.

[5] W. K. Chim, S. E. Leang, and D. S. H. Chan, "Extraction of metal-oxide semiconductor field-effect-transistor interface state and trapped charge spatial distributions using a physics-based algorithm," *Journ. Appl. Phys.*, vol. 81, no. 4, pp. 1992–1997, 1997.

[6] S. Mahapatra, C. Parikh, V. Rao, C. Viswanathan, and J. Vasi, "Device scaling effects on hot-carrier induced interface and oxide-trapped charge distributions in MOSFETs," *IEEE Trans. Electron Dev.*, vol. 47, no. 4, pp. 789–796, 2000.

[7] I. Starkov, S. Tyaginov, H. Enichlmair, J. Cervenka, C. Jungemann, S. Carniello, J. Park, H. Ceric, and T. Grasser, "Hot-carrier degradation caused interface state profile - simulations vs. experiment," *Journal of Vacuum Science and Technology - B*, vol. 29, no. 1, pp. 01AB09–1–01AB09–8, 2011.

[8] S. Tyaginov, I. Starkov, O. Triebl, H. Enichlmair, C. Jungemann, J. Park, H. Ceric, and T. Grasser, "Secondary generated holes as a crucial component for modeling of HC degradation in high-voltage n-MOSFET," in *Proc. International Conference on Simulation of Semiconductor Processes and Devices (SISPAD)*, 2011, pp. 123–126.

[9] S. Rauch and G. L. Rosa, "CMOS hot carrier: From physics to end of life projections, and qualification," in *Proc. International Reliability Physics Symposium (IRPS), tutorial*, 2010.

[10] I. Starkov, S. Tyaginov, H. Enichlmair, J. Park, T. Grasser, and C. Jungemann, "Analysis of worst-case hot-carrier degradation conditions in the case of n- and p-channel high-voltage MOSFETs," in *International Conference on Simulation of Semiconductor Processes and Devices (SISPAD)*, 2011, pp. 127–130.

[11] M. Houssa, M. Tuominen, M. Naili, V. Afanas'ev, A. Stesmans, S. Haukka, and M. M. Heyns, "Trap-assisted tunneling in high permittivity gate dielectric stacks," *Journ. Appl. Phys.*, vol. 87, no. 12, pp. 8615–8620, 2000.

[12] T. Grasser, "Stochastic charge trapping in oxides: From random telegraph noise to bias temperature instabilities," *Microelectronics Reliability*, vol. 52, no. 1, pp. 39–70, 2011.

[13] I. Starkov, H. Enichlmair, S. Tyaginov, and T. Grasser, "Analysis of the threshold voltage turn-around effect in high-voltage n-MOSFETs due to hot-carrier stress," in *Conference Proceedings of International Reliability Physics Symposium (IRPS 2012)*, 2012, pp. XT.7.1–XT.7.6.

[14] M. Tsuchiaki, H. Hara, T. Morimoto, H. Iwai, "A new charge pumping method for determining the spatial distribution of hot-carrier-induced fixed charge in p-MOSFET's," *IEEE Trans. Electron Dev.*, vol. 40, no. 10, pp. 1768–1799, 1993.

[15] S. Tyaginov, I. Starkov, O. Triebl, J. Cervenka, C. Jungemann, S. Carniello, J. Park, H. Enichlmail, C. Kernstock, E. Seebacher, R. Minixhofer, H. Ceric, and T. Grasser, "Interface traps density-of-states as a vital component for hot-carrier degradation modeling," *Microelectronics Reliability*, vol. 50, pp. 1267–1272, 2010.

[16] S. Chung and J.-J. Yang, "A new approach for characterizing structure-dependent hot-carrier effects in drain-engineered MOSFET's," *IEEE Trans. Electron Dev.*, vol. 46, no. 7, pp. 1371–1377, Jul. 1999.

[17] W. Chen, A. Q. Balasinski, and T. P. Ma, "Lateral profiling of oxide charge and interface traps near MOSFET junctions," *IEEE Trans. Electron Dev.*, vol. 40, no. 1, pp. 187–196, 1993.

[18] S. Okhonin, T. Hessler, and M. Dutoit, "Comparison of gate-induced drain leakage and charge pumping measurements for determining lateral interface trap profiles in electrically stressed MOSFETs," *IEEE Trans. Electron Dev.*, vol. 43, no. 4, pp. 605–612, 1996.

[19] I. Starkov, A. Starkov, S. Tyaginov, H. Enichlmair, H. Ceric, and T. Grasser, "An analytical model for MOSFET local oxide capacitance," in *Proc. International Semiconductor Device Research Symposium (ISDRS 2011)*, 2011.

[20] N. Pesonen, W. Kahn, R. Allen, M. Cresswell, and M. Zaghloul, "Application of conformal mapping approximation techniques: parallel conductors of finite dimensions," *IEEE Trans. Instrumentation and Measurement*, vol. 53, no. 3, pp. 812–821, june 2004.

[21] *MiniMOS-NT Device and Circuit Simulator*, Institute for Microelectronic, TU Wien.